

On Prats' problem with anomalous diffusion

Antonio Barletta 

Department of Industrial Engineering, Alma Mater Studiorum Università di Bologna,
Viale Risorgimento 2, 40136 Bologna, Italy

Corresponding author: Antonio Barletta, antonio.barletta@unibo.it

(Received 31 December 2025; revised 27 January 2026; accepted 27 February 2026)

The classical Prats problem of flow instability in a horizontal porous channel saturated by a fluid subject to a buoyancy force is reconsidered. In the original formulation, the driving buoyancy force results from thermal diffusion. This study, however, substitutes thermal diffusion with mass diffusion. Furthermore, the usual scheme of mass diffusion is extended to comprehend also the anomalous phenomena of superdiffusion and subdiffusion. Such phenomena are modelled via a time-dependent mass diffusivity which yields a significant change in the formulation of the stability eigenvalue problem. In particular, the ordinary differential equations governing the time evolution of the perturbations acting on the base throughflow become non-autonomous. This makes a significant difference in the discussion of the conditions leading to instability, with a marked effect of the anomaly in the mass diffusion process. The transition from convective to absolute instability for subdiffusion processes is also addressed.

Key words: buoyancy-driven instability, convection in porous media, absolute/convective instability

1. Introduction

The mechanism of mass diffusion in a fluid binary mixture is described on a microscopic scale as a molecular random walk (see, for example, Nelson 1967). The classical approach underlying the so-called normal mass diffusion is based on a very special relation between the variance, σ_x^2 , of the solute molecular position, $\mathbf{x}(t)$, and time, t . In fact, normal mass diffusion means a proportionality relation at large times

$$\sigma_x^2 \sim D t, \quad (1.1)$$

where D is the mass diffusivity coefficient: a time-independent property of the binary mixture. Anomalous, or fractional, mass diffusion occurs when the behaviour of the random walk at large times means a departure from the proportionality law (1.1). Several

studies and reviews have been published in the last decades regarding the physics and the mathematical modelling of anomalous diffusion (Metzler & Klafter 2000; Gorenflo *et al.* 2002*a,b*; Wu & Berland 2008; Henry *et al.* 2010; dos Santos 2019; Cai *et al.* 2025). The two ways where the large-time behaviour described by (1.1) may become anomalous is through a faster spreading process of the molecular distribution, i.e. superdiffusion, or through a slower spreading process, i.e. subdiffusion. Thus, a usual model of anomalous diffusion is based on a power law where (1.1) is actually replaced by

$$\sigma_x^2 \sim \mathcal{D}(t) t \quad \text{for} \quad \mathcal{D}(t) \sim t^{r-1}. \quad (1.2)$$

Here, r is a positive index of anomalous diffusion. The special case $r = 1$ means normal diffusion, with (1.2) becoming equivalent to (1.1), while $r > 1$ defines superdiffusion and $0 < r < 1$ defines subdiffusion. As pointed out, for example, in Barletta *et al.* (2025*a*) and in Barletta *et al.* (2025*b*), the power law is just a special case of what the large time behaviour of the diffusivity can be for either subdiffusion or superdiffusion, whereas a more general definition will be adopted later on, in § 5 of this paper, with (5.12). We refer the reader to the previous literature on the topic for specific assessments of the molecular dynamics that explain the reasons for the emergence of superdiffusive or subdiffusive processes.

The aim of this paper is to take another step forward in the understanding of the interplay between anomalous mass diffusion and the emergence of buoyancy-induced flow instability and convection in a fluid saturated porous medium. This important subject was first investigated by Karani *et al.* (2017) and by Klimenko & Maryshev (2017). In those papers, anomalous diffusion is modelled via fractional differential operators. The authors either adopted a fractional-order advective term (Karani *et al.* 2017) in the diffusion equation or they subdivided the solute concentration into mobile and immobile phases linked by a kinetic equation involving a fractional time derivative (Klimenko & Maryshev 2017). Novel investigations of the Horton–Rogers–Lapwood problem (Horton & Rogers Jr 1945; Lapwood 1948), namely the onset of the Rayleigh–Bénard instability in a fluid saturated horizontal porous layer, were recently proposed by Barletta (2023) and by Straughan & Barletta (2024). Up to this point, the analysis of the buoyancy-induced instability has only been developed for an equilibrium state of the fluid system where the seepage velocity is zero. The variant formulation of the Horton–Rogers–Lapwood problem, where a uniform horizontal throughflow occurs at equilibrium, is investigated in the pioneering paper by Prats (1966) and, after that study, it is now well known as Prats’ problem (Cheng 1978; Nield & Bejan 2017).

The objective of the present study is to extend the analysis of Prats’ problem, classically carried out for normal diffusion, with conditions where anomalous diffusion occurs. The Péclet number, which parametrises the throughflow rate, introduces an oscillatory pattern to the temporal evolution of the perturbations. The concurrent evolution of their amplitude then may lead the flow toward either stability or instability. Furthermore, the onset of instability is mainly influenced by the anomaly, superdiffusion or subdiffusion, and by the Rayleigh number for the cases of normal diffusion or subdiffusion. The possibility to detect the growing amplitude of the unstable perturbations in a laboratory reference frame is also discussed by investigating the transition from convective to absolute instability with special reference to the case of subdiffusion.

2. Experimental evidence and different frameworks of anomalous diffusion

Studies presenting experimental evidence for anomalous diffusion are relatively abundant in the literature. Ren *et al.* (1992) employed a dynamic light scattering technique to

investigate the molecular relaxation modes of polymer solutions. In particular, they used aqueous solutions of gelatin. These authors revealed molecular random walk scenarios with mean-squared displacement of the diffusing molecules, i.e. the variance σ_x^2 , expressed with either logarithmic or power-law functions of time at different time intervals. Actually, they found evidence for a subdiffusive dynamics of the solute molecules. Tolić-Nørrelykke *et al.* (2004) proposed observational evidence of anomalous diffusion in biofluids by image analysis of granules diffusing in a yeast cell. By multiple particle tracking, they found mean-squared displacements of granules following a power law in time with an anomalous exponent r around 0.75, showing subdiffusion. Gal & Weihs (2010) used fluorescent carboxyl-coated polystyrene probe particles for the analysis of the diffusion dynamics in living cells, demonstrating superdiffusive behaviour with a power-law exponent approximately equal to 1.25. Jeon *et al.* (2013) reported a very strong subdiffusive dynamics, with a power-law exponent $r \approx 0.3$, from single particle tracking of polystyrene microbeads in a micellar solution. These authors adopted optical tweezers and a video tracking technique to observe the evolution in time of the microbeads' mean-squared displacement.

Besides the area of biofluids, observations of anomalies in the diffusion process were observed for shear flows. For example, Orihara & Takikawa (2011) carried out an experiment with micron or submicron solid particles (polystyrene spheres) undergoing diffusion in a water or glycerine shear flow. The mean-squared displacements were measured by a confocal scanning laser microscope and revealed superdiffusion with a power-law exponent $r \approx 3$. Orihara & Takikawa (2011) concluded that the anomalous diffusion of the microparticles is 'caused by the coupling between the normal diffusion along the velocity gradient and the convection', thus revealing an active role of the solvent fluid flow in determining the anomaly. Correlated to such an experiment is the study of sediment flux in rivers carried out by Martin, Jerolmack & Schumer (2012). The study was conducted by tracing the trajectories of gravel particles along a laboratory flume and revealed superdiffusion with r approximately equal to 1.6 at earlier times and 1.4 at larger times. The key mechanism behind the superdiffusion statistics of the random walk is the occasional emergence of the so-called Levy flights, intended as long time intervals where the diffusing particle does not undergo any collision. Levy flights are responsible for the departure from normal diffusion by altering the statistics of the random walk. On the opposite side, subdiffusion is often associated with such mechanisms as particle trapping, which may occur especially when the solvent flow is seepage in a porous solid material.

The logical steps linking the random walk analysis to the continuous model based on a mass diffusion equation may be taken by starting with a Langevin equation for the description of the random walk dynamics. Then, the statistics inferred from the Langevin equation are transferred to a master equation for the probability distribution of the diffusing particles. Finally, the master equation serves to formulate the mass diffusion equation. Such steps are thoroughly described, for instance, by Henry *et al.* (2010). The formulations of the macroscopic mass diffusion equation available in the literature usually differ by the presence of a time fractional-derivative term or of a fractional-Laplacian term. Fractional derivatives are also absent in some models, but a time-dependent or space-dependent mass diffusivity coefficient is present instead (Metzler & Klafter 2000; Henry *et al.* 2010). The emergence of a fractional-derivative formulation of the mass diffusion equation is often a consequence of a fractional-derivative model for the starting Langevin equation, which describes the random walk. A simplified treatment of the logical steps leading to a mass diffusion equation without fractional derivatives and with a time-dependent mass diffusivity coefficient can be found in Barletta (2023) and in Barletta *et al.* (2025b). To the best of author's knowledge, there are no profound physical arguments,

to date, leading to a choice between fractional-derivative and variable-diffusivity models of anomalous diffusion. When anomalous diffusion is treated in conjunction with flow stability problems, as in the present paper, the use of fractional-derivative approaches may lead to the need for some extra parameters beyond the mere power-law index r . A similar circumstance has been pointed out in Barletta (2023), where the analysis of the Rayleigh–Bénard instability in a porous layer has been carried out both with a time-dependent diffusivity model and with a fractional-derivative model. The results differ in terms of the neutral stability condition. In particular, the threshold to instability predicted via the fractional-derivative model strongly depends on an extra parameter. Such a parameter is a dimensionless relaxation time, which should be determined experimentally (Barletta 2023). However, differently from the power-law index r , the values of the relaxation time are not available in the literature, so that the comparison between the predictions of different models is complicated. A way out of such an uncertainty is a direct experimental study of the Rayleigh–Bénard instability with an anomalous diffusion process, which is definitely an interesting challenge for future developments of the research on this topic.

3. Mathematical model

Let us consider a horizontal porous channel saturated by a fluid binary mixture with C the concentration of the solute, \mathbf{u} the fluid seepage velocity and P the local difference between the pressure and the hydrostatic pressure. The Cartesian components of \mathbf{u} are (u, v, w) along the (x, y, z) axes. The buoyancy force acts on the fluid as described through the Oberbeck–Boussinesq approximation (Straughan 2008; Nield & Bejan 2017; Barletta 2022), where the local momentum balance equation is written according to Darcy’s law

$$\begin{aligned} \nabla \cdot \mathbf{u} &= 0, \\ \frac{\mu}{K} \mathbf{u} &= -\nabla P - \rho_0 \beta (C - C_0) \mathbf{g}, \\ \varphi \frac{\partial C}{\partial t} + \mathbf{u} \cdot \nabla C &= \varphi \mathcal{D}(t) \nabla^2 C. \end{aligned} \quad (3.1)$$

In (3.1), the anomalous diffusion is modelled via a time-dependent mass diffusivity, $\mathcal{D}(t)$ (Henry *et al.* 2010; Liang *et al.* 2021; Barletta *et al.* 2025a,b; Girelli *et al.* 2025). The properties μ , K , β , φ and ρ_0 are the dynamic viscosity, permeability, expansion coefficient relative to mass diffusion, porosity and fluid density evaluated when the solute concentration has the reference value C_0 . The gravitational acceleration \mathbf{g} is uniform and parallel to the z axis, so that $\mathbf{g} = -g \mathbf{e}_z$, with g the modulus of \mathbf{g} and \mathbf{e}_z the unit vector of the z axis.

An important point is that the mathematical model (3.1) is formulated by assuming an isotropic permeability K and diffusivity \mathcal{D} . This is a special case of a general formulation where both K and \mathcal{D} should be second-order tensors describing a possible anisotropy of the seepage flow and of the mass diffusion process. Furthermore, (3.1) is local both in time and in space, meaning that all terms are evaluated at a single instant of time and at a single position in space. Locality coincides with the so-called quasi-steady approximation (Valdés-Parada & Sánchez-Vargas 2024) where the envisaged general case involves time convolutions in order to model relaxation phenomena which, in the present model given by (3.1), are neglected. Relaxation phenomena and non-locality are also typical of fractional-derivative models. In fact, fractional derivatives and differential operators, despite their names, are integral quantities involving the time history of the process and the spatial extent where the process occurs.

The horizontal porous channel is confined by the horizontal impermeable planes, $z = 0$ and $z = L$, kept at constant uniform concentrations C_1 and C_2 , respectively. Thus, a reasonable choice of the reference concentration C_0 is the arithmetic average $(C_1 + C_2)/2$. Let \mathcal{D}_0 be a conveniently chosen reference value of the time-dependent mass diffusivity. In the special case of normal diffusion, we choose the reference value \mathcal{D}_0 as the limit of $\mathcal{D}(t)$ when $t \rightarrow +\infty$. The governing equations (3.1) and their boundary conditions can be rendered dimensionless through the assignment of suitable scaling constants, namely

$$\begin{aligned} \frac{(x, y, z)}{L} &\rightarrow (x, y, z) & \frac{t}{L^2/\mathcal{D}_0} &\rightarrow t & \frac{\mathbf{u}}{\varphi \mathcal{D}_0/L} &\rightarrow \mathbf{u}, \\ \frac{P}{\varphi \mu \mathcal{D}_0/K} &\rightarrow P & \frac{C - C_0}{C_1 - C_2} &\rightarrow C & \frac{\mathcal{D}(t)}{\mathcal{D}_0} &\rightarrow \mathcal{D}(t). \end{aligned} \tag{3.2}$$

We can now reformulate the governing equations in dimensionless terms as

$$\begin{aligned} \nabla \cdot \mathbf{u} &= 0, \\ \mathbf{u} &= -\nabla P + Ra C \mathbf{e}_z, \\ \frac{\partial C}{\partial t} + \mathbf{u} \cdot \nabla C &= \mathcal{D}(t) \nabla^2 C. \end{aligned} \tag{3.3}$$

The mass diffusion Rayleigh number employed in (3.3) is defined as

$$Ra = \frac{\rho_0 \beta g (C_1 - C_2) K L}{\varphi \mu \mathcal{D}_0}. \tag{3.4}$$

The dimensionless boundary conditions can be expressed as

$$\begin{aligned} z = 0: & \quad w = 0 \quad C = \frac{1}{2}, \\ z = 1: & \quad w = 0 \quad C = -\frac{1}{2}. \end{aligned} \tag{3.5}$$

4. The stationary throughflow

The Prats problem is a variant of the Rayleigh–Bénard problem for a saturated porous medium where the basic state features a steady horizontal throughflow. In fact, a basic solution of (3.3) and (3.5), denoted with the subscript b , is given by

$$\mathbf{u}_b = (Pe, 0, 0) \quad C_b = \frac{1}{2} - z \quad \nabla P_b = (-Pe, 0, Ra C_b). \tag{4.1}$$

The basic solution (4.1) is parametrised by the Péclet number, Pe , expressing the prescribed horizontal flow rate. More precisely, the Péclet number serves to express the ratio between the dimensional reference velocity of the fluid flow and the dimensional diffusion characteristic velocity, i.e. $\varphi \mathcal{D}_0/L$. In Prats’ problem, the dimensional reference velocity is the velocity in the stationary throughflow. Hence, from the definition of the velocity scale employed for the dimensionless formulation, Pe is the dimensionless velocity in the x direction for the stationary throughflow.

5. Linear convective instability

The linear convective instability of the basic throughflow (4.1) can be tested by superposing small-amplitude perturbations defined as

$$\mathbf{u} = \mathbf{u}_b + \epsilon \hat{\mathbf{u}} \quad C = C_b + \epsilon \hat{C} \quad \nabla P = \nabla P_b + \epsilon \nabla \hat{P} \quad \text{for } |\epsilon| \ll 1. \tag{5.1}$$

With (5.1), by neglecting terms $\mathcal{O}(\epsilon^2)$, we can rewrite (3.3) and (3.5) as

$$\begin{aligned} \nabla \cdot \hat{\mathbf{u}} &= 0, \\ \hat{\mathbf{u}} &= -\nabla \hat{P} + Ra \hat{C} \mathbf{e}_z, \\ \frac{\partial \hat{C}}{\partial t} - \hat{w} + Pe \frac{\partial \hat{C}}{\partial x} &= \mathcal{D}(t) \nabla^2 \hat{C}, \end{aligned} \tag{5.2}$$

with

$$z = 0, 1: \quad \hat{w} = 0 \quad \hat{C} = 0. \tag{5.3}$$

A pressure–concentration reformulation of (5.2) and (5.3) is obtained by evaluating the divergence of the second (5.2), namely

$$\begin{aligned} \nabla^2 \hat{P} - Ra \frac{\partial \hat{C}}{\partial z} &= 0, \\ \frac{\partial \hat{C}}{\partial t} + \frac{\partial \hat{P}}{\partial z} - Ra \hat{C} + Pe \frac{\partial \hat{C}}{\partial x} &= \mathcal{D}(t) \nabla^2 \hat{C}, \end{aligned} \tag{5.4}$$

with

$$z = 0, 1: \quad \frac{\partial \hat{P}}{\partial z} = 0 \quad \hat{C} = 0. \tag{5.5}$$

The strategy to solve the stability problem expressed by (5.4) and (5.5) is based on the use of normal modes

$$\hat{P} = f(t) \cos(n\pi z) e^{i(k_x x + k_y y)} \quad \hat{C} = h(t) \sin(n\pi z) e^{i(k_x x + k_y y)}, \tag{5.6}$$

where n is a positive integer, $\mathbf{k} = (k_x, k_y, 0)$ is the horizontal wave vector and k is the wavenumber, such that $k^2 = k_x^2 + k_y^2$. Equation (5.6) satisfies the boundary conditions (5.5) for every n and \mathbf{k} , while (5.4) are satisfied if

$$f(t) = -\frac{n\pi Ra}{n^2\pi^2 + k^2} h(t), \tag{5.7}$$

and

$$\frac{d}{dt} \log[h(t)] = \frac{k^2 Ra}{n^2\pi^2 + k^2} - (n^2\pi^2 + k^2) \mathcal{D}(t) - i k_x Pe. \tag{5.8}$$

One can easily obtain the solution of (5.8)

$$h(t) = h(0) e^{(n^2\pi^2 + k^2) G(t)} e^{-i k_x Pe t}, \tag{5.9}$$

where

$$G(t) = \frac{k^2 Ra}{(n^2\pi^2 + k^2)^2} t - \int_0^t \mathcal{D}(t') dt'. \tag{5.10}$$

What determines the ultimate effect of the perturbations superposed to the basic flow is the limit of $G(t)$ when $t \rightarrow +\infty$. In fact, we have three possible cases

$$\lim_{t \rightarrow +\infty} G(t) = \begin{cases} +\infty & \text{instability,} \\ 0 & \text{neutral stability,} \\ -\infty & \text{stability.} \end{cases} \tag{5.11}$$

Which of the three cases actually occurs depends strongly on the type of diffusion

$$\lim_{t \rightarrow +\infty} \frac{1}{t} \int_0^t \mathcal{D}(t') dt' = \begin{cases} +\infty & \text{superdiffusion,} \\ 1 & \text{normal diffusion,} \\ 0 & \text{subdiffusion,} \end{cases} \quad (5.12)$$

where, for normal diffusion, the value 1 is a consequence of the scaling employed for the dimensionless formulation (3.2) and of the declared choice of the dimensional reference diffusivity \mathcal{D}_0 . On account of (5.10)–(5.12), one may conclude that neutral stability is only possible for subdiffusion with $Ra = 0$, or for normal diffusion provided that

$$Ra = \frac{(n^2 \pi^2 + k^2)^2}{k^2}. \quad (5.13)$$

Stability occurs either for superdiffusion independently of the Rayleigh number, for subdiffusion with $Ra < 0$, or for normal diffusion with

$$Ra < \frac{(\pi^2 + k^2)^2}{k^2}. \quad (5.14)$$

Finally, instability takes place with subdiffusion for every positive Rayleigh number, or with normal diffusion when

$$Ra > \frac{(\pi^2 + k^2)^2}{k^2}. \quad (5.15)$$

One can reckon that, for subdiffusion, any arbitrarily weak destabilising concentration gradient leads to convective instability.

It is important to point out that, even if the onset of instability is determined by the asymptotic behaviour defined by the limiting condition (5.12), the characteristics of the whole evolution in time of $\mathcal{D}(t)$ may conceal or delay the actual observation of instability within a finite time experiment.

Equation (5.7) shows that the eigenfunctions, $f(t)$ and $h(t)$, are determined so that the initial values $f(0)$ and $h(0)$ must be linked in a special way. On the other hand, (5.9) forces the modulus of the eigenfunctions to evolve in time independently of the Péclet number and, hence, of the throughflow rate in the basic state (4.1). As a consequence, the stable/unstable nature of the basic state is exactly the same as in the analysis of the anomalous Horton–Rogers–Lapwood problem carried out by Barletta (2023). The only difference is in the phase factor $\exp(-ik_x Pe t)$ displayed in (5.9). This term influences the ultimate asymptotic growth or decay of the perturbation amplitudes with an oscillatory behaviour. In practice, such oscillations are quite important, as they may hinder the possibility to detect, with a laboratory experiment, the actual growth of the perturbation amplitude with a measurement taken at a given spatial position in the streamwise direction x . This argument gives the Péclet number a central role in establishing experimentally the onset of instability. This aspect of the Prats problem, in the case of normal diffusion, is pointed out in Delache, Ouarzazi & Combarous (2007) and in the book by Barletta (2019). The effect of oscillations is grounded on the value of $k_x Pe$, so that this effect is maximum for transverse waves ($k_x = k, k_y = 0$), while it gradually decreases for oblique waves and, eventually, vanishes with longitudinal waves ($k_x = 0, k_y = k$). This well-known feature of flow instability results in the distinction between convective and absolute instability (Carriere & Monkewitz 1999; Suslov 2006; Delache *et al.* 2007; Barletta 2019). As explained in the literature relative to normal diffusion, absolute instability is possible for supercritical conditions, i.e. when we are above the neutral stability threshold and Ra exceeds a value, Ra_{abs} , that monotonically increases with Pe . Only when absolute

instability occurs is an observer in a reference frame at rest able to detect experimentally a perturbation amplifying in place and, hence, an unstable behaviour of the basic flow. In the forthcoming section, an extension of the methodology underlying the absolute instability analysis for processes of subdiffusion is presented in order to establish whether the predicted convective instability for $Ra > 0$ also implies absolute instability or not.

The modes with $n > 1$ do not contribute in any practical way to the dynamics of instability (either convective or absolute). In fact, the modes with $n = 1$ yield in every case, and in particular for subdiffusion, the lowest threshold value of Ra for instability. Higher n thresholds certainly exist, according to the linear analysis, but they emerge within a supercritical regime. In this regime, the perturbation amplitude amplification already occurs, caused by the $n = 1$ modes. As a consequence, in the supercritical regime, the perturbation dynamics is intrinsically nonlinear due to the increasingly large amplitude of the perturbations. Thus, the predicted $n > 1$ thresholds mathematically exist, but they are physically impractical.

6. Absolute instability for subdiffusion

We follow the method described in Chapter 8 of the book by Barletta (2019), and consider a wavepacket perturbation given by a superposition of normal modes defined by (5.6), (5.7) and (5.9). We consider a given horizontal direction of the normal modes, defined by an angle ϕ such that

$$\mathbf{k} = (k \cos \phi, k \sin \phi, 0). \tag{6.1}$$

One may reckon from (5.10) and (5.12), that, for subdiffusion, a large-time approximation of $G(t)$ is

$$G(t) \approx \frac{k^2 Ra}{(n^2 \pi^2 + k^2)^2} t. \tag{6.2}$$

Then, a wavepacket propagating along such a direction is described by the Fourier integral

$$\hat{C}(x, y, z, t) = \frac{1}{\sqrt{2\pi}} \int_{-\infty}^{+\infty} A_{n,k}(x, y, z) e^{\lambda(k)t} dk, \tag{6.3}$$

where

$$A_{n,k}(x, y, z) = h(0) \sin(n\pi z) e^{ik(x \cos \phi + y \sin \phi)}, \tag{6.4}$$

and

$$\lambda(k) = \frac{k^2 Ra}{n^2 \pi^2 + k^2} - ikPe \cos \phi. \tag{6.5}$$

It can be mentioned that a similar wavepacket expression applies also to $\hat{P}(x, y, z, t)$ with just two differences in the definition of $A_{n,k}(x, y, z)$: $f(0)$ must be used instead of $h(0)$ and $\cos(n\pi z)$ must be used instead of $\sin(n\pi z)$. We can now develop the steepest descent approximation for the wavepacket $\hat{C}(x, y, z, t)$ having in mind that the same outcome applies also to $\hat{P}(x, y, z, t)$ as it is based just on the coefficient $\lambda(k)$, which is common to both wavepackets. We have to determine the complex zeros, k_0 , of the derivative $d\lambda(k)/dk$, i.e. the saddle points. Thus, the saddle points, $k = k_0$, can be expressed in terms of the complex roots, γ , of

$$\frac{2\gamma X}{(1 + \gamma^2)^2} = i \quad \text{for} \quad \gamma = \frac{k}{n\pi} \quad X = \frac{Ra}{n\pi Pe \cos \phi}. \tag{6.6}$$

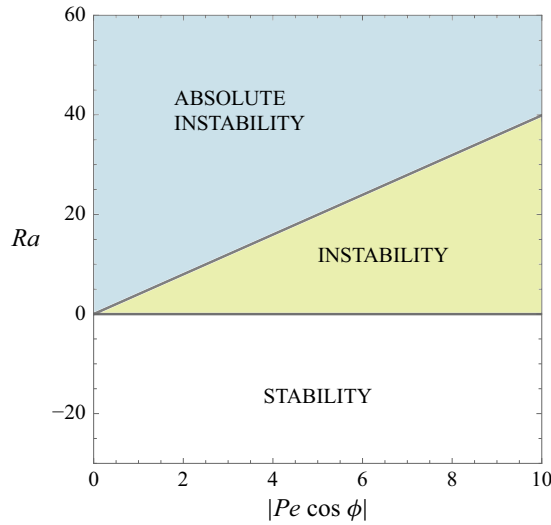


Figure 1. Subdiffusion: drawing of the linear stability, instability and absolute instability regions in the $(|Pe \cos \phi|, Ra)$ parametric plane. The white region corresponds to stability, the yellow region to instability and the blue region to absolute instability.

By solving (6.6), one can determine the saddle points for every given value of X . If we aim to determine the threshold $X = X_{abs}$ to absolute instability, then the solution of (6.6) must be sought so that $\text{Re}(\lambda(k_0)) = 0$, where Re and Im stand for the real and imaginary parts of a complex variable. Such an additional constraint allows one to determine both the saddle points k_0 and the value of X_{abs} , namely

$$\begin{aligned} k_0/(n\pi) &= \pm 0.8337830 - 1.041913 i & X_{abs} &= 1.270325, \\ k_0/(n\pi) &= \pm 0.8337830 + 1.041913 i & X_{abs} &= -1.270325. \end{aligned} \tag{6.7}$$

Given that the threshold value of the Rayleigh number for the onset of absolute instability cannot be negative, $Ra_{abs} \geq 0$, while there are no restrictions on the sign of $Pe \cos \phi$, both the symmetric values of X_{abs} given by (6.7) are meaningful. We can conclude that absolute instability for subdiffusion occurs when Ra exceeds a threshold, Ra_{abs} , that can be expressed as

$$Ra_{abs} = 1.270325 n\pi |Pe \cos \phi|. \tag{6.8}$$

Then, the least Rayleigh number conditions for absolute instability corresponding to a prescribed Péclet number are achieved with $n = 1$ and $\cos \phi = 0$, namely with longitudinal modes, $\phi = \pi/2$ or $\mathbf{k} = (0, k, 0)$. On the other hand, the largest threshold Ra_{abs} to absolute instability corresponds to transverse modes, $\phi = 0$ or $\mathbf{k} = (k, 0, 0)$. This result makes perfect sense as longitudinal modes grow in place so that they are not convected downstream by the basic throughflow. Stated differently, the time evolution of the longitudinal modes is unaffected by the oscillatory phase factor, $\exp(-ik_x Pet)$, displayed in (5.9).

Figure 1 illustrates the results of the linear stability analysis for subdiffusion as they emerge from the arguments presented in § 5 and from the evaluation of the absolute instability threshold given by (6.8) with $n = 1$.

Figure 2 shows graphically that the so-called holomorphy requirement (Suslov 2006; Barletta 2019) is satisfied by the saddle points given by (6.7). This means that one can

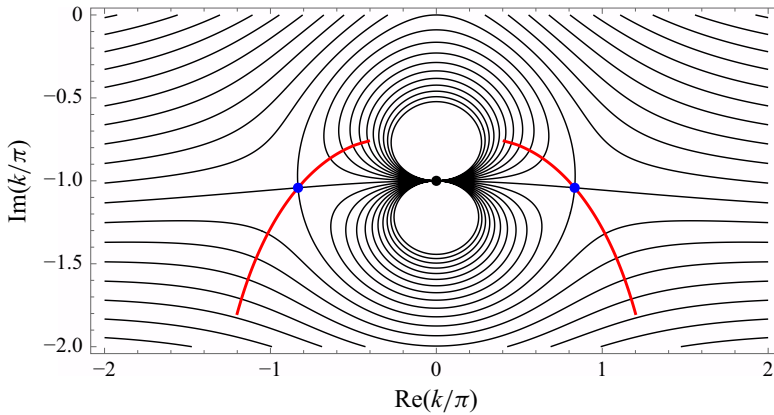


Figure 2. Check of the holomorphy requirement in the complex k plane, for $Ra = Ra_{abs}$, $n = 1$ and $Pe \cos \phi > 0$. The black lines are the isolines of $\text{Re}(\lambda(k))$. The blue dots correspond to the saddle points $k = k_0$, while the central black dot denotes the singularity $k = -i\pi$. The red lines show the paths of steepest descent for $\text{Re}(\lambda(k))$ crossing the saddle points.

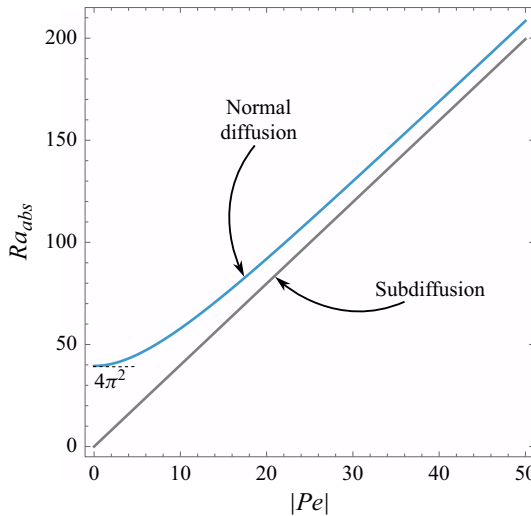


Figure 3. Transverse modes ($\phi = 0$) with $n = 1$: comparison between the absolute instability threshold for normal diffusion (Delache *et al.* 2007; Barletta 2019) and that for subdiffusion, showing up the earlier onset of absolute instability under subdiffusion. The black line corresponds to the threshold value Ra_{abs} versus $|Pe|$ for subdiffusion. The blue line corresponds to the threshold value Ra_{abs} versus $|Pe|$ for normal diffusion.

continuously deform the integration domain for the right-hand side of (6.3), namely the line $\text{Im}(k) = 0$, into a curve crossing the saddle points through a path which is locally of steepest descent for $\text{Re}(\lambda(k))$. Such paths of steepest descent are displayed in figure 2 as red lines. The blue dots are the saddle points, while the black dot is the singularity $k = -i\pi$. The saddle points are at the intersections of the isolines $\text{Re}(\lambda(k)) = 0$. The union of the deformed path crossing the saddle points and the original integration path, $\text{Im}(k) = 0$, must yield a contour that does not contain any singularity of $\text{Re}(\lambda(k))$. Figure 2 demonstrates that the latter statement holds true or, equivalently, that the holomorphy requirement can be satisfied.

Figure 3 displays a comparison between the trends of Ra_{abs} for the case of transverse modes with normal diffusion (data reported by Delache *et al.* (2007) and Barletta (2019))

$ Pe $	Ra_{abs} for subdiffusion	Ra_{abs} for normal diffusion
0	0.0000	39.4784
10	39.9084	57.8036
20	79.8169	91.9528
50	199.542	208.441
100	399.084	407.140

Table 1. Values of Ra_{abs} versus $|Pe|$ for $n = 1$ and $\phi = 0$ with either subdiffusion or normal diffusion.

with (6.8) for subdiffusion. One can conclude that the transition to absolute instability for normal diffusion requires larger values of Ra than for subdiffusion, for every fixed value of Pe . As suggested by figure 3, for large values of Pe , the difference, ΔRa_{abs} , between Ra_{abs} for normal diffusion and subdiffusion tends to an asymptotic value that can be evaluated by employing Richardson’s extrapolation, namely $\Delta Ra_{abs} \approx 7.3356$. A common feature of normal diffusion and subdiffusion displayed in figure 3 is that, with $Pe = 0$, the transition to absolute instability takes place at critical conditions without any gap in Ra , i.e. with $Ra = Ra_c = 4\pi^2$ for normal diffusion and $Ra = Ra_c = 0$ for subdiffusion. Table 1 shows some representative values of Ra_{abs} versus $|Pe|$ for subdiffusion and for normal diffusion with $n = 1$ and $\phi = 0$. Such values could serve as benchmark data for future theoretical and numerical studies of this problem.

7. Conclusions

The anomalous diffusion effects on the onset of instability in a horizontal porous channel flow have been investigated. The mechanism of instability relies on the interplay between the mass diffusion and buoyancy force as modelled through the Oberbeck–Boussinesq approximation. The model adopted is based on Darcy’s law of momentum transfer and on a mass diffusion equation accounting both for advection and for the anomalous diffusion phenomenon, through a time-dependent diffusivity coefficient. The instability for the equilibrium solution of the local balance governing equations has been tested. The equilibrium solution is a basic state of stationary flow with a uniform seepage velocity in a horizontal direction and a uniform vertical concentration gradient. Perturbations superposed on such an equilibrium state have been defined as normal modes with a given dimensionless wave vector along any horizontal direction. The transition to instability is governed by the Rayleigh number, Ra , and the Péclet number, Pe . The main findings can be summarised as follows:

- (i) Superdiffusion, modelled as a process where the mass diffusivity averaged over a large time diverges to infinity, leads to a decay in time of the perturbation amplitudes, for every real value of Ra and for every real value of Pe , and hence to stability.
- (ii) Subdiffusion, modelled as a process where the mass diffusivity averaged over a large time tends to zero, leads to an amplification in time of the perturbation amplitudes, for every positive Ra and for every real value of Pe , and hence to instability. With $Ra = 0$, subdiffusion leads to neutral stability and, with $Ra < 0$, to stability.
- (iii) For normal diffusion, modelled as a process where the mass diffusivity averaged over a large time tends to a non-zero constant, we recover exactly the same results described in the paper by Prats (1966) and reviewed in Cheng (1978) and Nield & Bejan (2017).

- (iv) The non-zero throughflow envisaged in the basic equilibrium state, parametrised through the Péclet number, yields an oscillatory trend to the amplification or decay of the perturbation amplitude for either transverse or oblique modes.
- (v) Transition to absolute instability for subdiffusion occurs for $Ra > Ra_{abs}$ with Ra_{abs} directly proportional to $|Pe|$. For every fixed Pe , the transition to absolute instability occurs at lower Rayleigh numbers for subdiffusion than for normal diffusion.

The conditions for the onset of linear instability are exactly the same as those described by Barletta (2023) relative to the anomalous Horton–Rogers–Lapwood problem, which is the special case of Prats’ problem where the Péclet number is zero. Barletta (2023) presented a comparison with the conditions for instability predicted according to a fractional-derivative model of subdiffusion. The comparison revealed that the onset of instability predicted via the fractional-derivative model depends on an advection-mobility dimensionless parameter which is absent in the model based on a time-dependent diffusivity employed in this study.

There are several opportunities for future developments of the research on anomalous diffusion and the instability of flows. In fact, the analysis of the anomalous Prats problem is a mathematically simple application, while more complicated situations may emerge for the Navier–Stokes shear flows with mass diffusion. For instance, the emergence of an interplay between the hydrodynamic instability and the anomalous diffusion phenomenology may display novel features for the so-called Rayleigh–Bénard–Poiseuille problem.

Acknowledgements. This work was financially supported by Alma Mater Studiorum Università di Bologna, grant number RFO-2025.

Declaration of interests. The author reports no conflicts of interest.

REFERENCES

- BARLETTA, A. 2019 *Routes to Absolute Instability in Porous Media*. Springer.
- BARLETTA, A. 2022 The Boussinesq approximation for buoyant flows. *Mech. Res. Commun.* **124**, 103939.
- BARLETTA, A. 2023 Rayleigh–Bénard instability in a horizontal porous layer with anomalous diffusion. *Phys. Fluids* **35**, 104114.
- BARLETTA, A., BRANDÃO, P.V., CAPONE, F. & DE LUCA, R. 2025a Stabilizing effect of generic anomalous diffusion independent of the Rayleigh number. *Intl Commun. Heat Mass* **168**, 109410.
- BARLETTA, A., REES, D.A.S., CELLI, M. & BRANDÃO, P.V. 2025b Open boundaries, anomalous diffusion and the Darcy–Bénard instability. *Transp. Porous Med.* **152**, 27.
- CAI, W., HU, Y., QU, X., ZHAO, H., WANG, G., LI, J. & HUANG, Z. 2025 Machine learning analysis of anomalous diffusion. *Eur. Phys. J. Plus* **140**, 183.
- CARRIERE, P. & MONKEWITZ, P.A. 1999 Convective versus absolute instability in mixed Rayleigh–Bénard–Poiseuille convection. *J. Fluid Mech.* **384**, 243–262.
- CHENG, P. 1978 Heat transfer in geothermal systems. In *Advances in Heat Transfer*, vol. 14, pp. 1–105. Academic Press.
- DELACHE, A., OUARZAZI, M.N. & COMBARNOUS, M. 2007 Spatio-temporal stability analysis of mixed convection flows in porous media heated from below: comparison with experiments. *Intl J. Heat Mass Transfer* **50**, 1485–1499.
- DOS SANTOS, M.A.F. 2019 Analytic approaches of the anomalous diffusion: a review. *Chaos Solitons Fractals* **124**, 86–96.
- GAL, N. & WEIHS, D. 2010 Experimental evidence of strong anomalous diffusion in living cells. *Phys. Rev. E - Statist. Nonlinear Soft Matter Phys.* **81**, 020903.
- GIRELLI, A., GIANTESIO, G., MUSESTI, A. & PENTA, R. 2025 Dynamical anomalous transport of molecules subject to inhomogeneous body forces. *Zeitschrift für Angewandte Mathematik und Physik* **76**, 249.
- GORENFLO, R., MAINARDI, F., MORETTI, D., PAGNINI, G. & PARADISI, P. 2002a Discrete random walk models for space-time fractional diffusion. *Chem. Phys.* **284**, 521–541.

- GORENFLO, R., MAINARDI, F., MORETTI, D. & PARADISI, P. 2002*b* Time fractional diffusion: a discrete random walk approach. *Nonlinear Dyn.* **29**, 129–143.
- HENRY, B.I., LANGLANDS, T.A.M. & STRAKA, P. 2010 An introduction to fractional diffusion. In *Complex Physical, Biophysical and Econophysical Systems* (ed. R.L Dewar & F. Detering), pp. 37–89. World Scientific.
- HORTON, C.W. & ROGERS, F.T.Jr 1945 Convection currents in a porous medium. *J. Appl. Phys.* **16** (6), 367–370.
- JEON, J.-H., LEIJNSE, N., ODDERSHEDE, L.B. & METZLER, R. 2013 Anomalous diffusion and power-law relaxation of the time averaged mean squared displacement in worm-like micellar solutions. *New J. Phys.* **15**, 045011.
- KARANI, H., RASHTBEHESHT, M., HUBER, C. & MAGIN, R.L. 2017 Onset of fractional-order thermal convection in porous media. *Phys. Rev. E* **96**, 063105.
- KLIMENKO, L.S. & MARYSHEV, B.S. 2017 Effect of solute immobilization on the stability problem within the fractional model in the solute analog of the Horton-Rogers-Lapwood problem. *Eur. Phys. J. E* **40**, 1–7.
- LAPWOOD, E.R. 1948 Convection of a fluid in a porous medium. *Math. Proc. Camb.* **44**, 508–521.
- LIANG, Y., TIAN, P., WANG, S. & XU, W. 2021 Non-Fickian diffusion in time–space fluctuating diffusivity landscapes: from superfast to ultraslow. *Fractals* **29**, 2150191.
- MARTIN, R.L., JEROLMACK, D.J. & SCHUMER, R. 2012 The physical basis for anomalous diffusion in bed load transport. *J. Geophys. Res.: Earth Surface* **117**, F01018.
- METZLER, R. & KLAFTER, J. 2000 The random walk’s guide to anomalous diffusion: a fractional dynamics approach. *Phys. Rep.* **339**, 1–77.
- NELSON, E. 1967 *Dynamical Theories of Brownian Motion*. Princeton University Press.
- NIELD, D.A. & BEJAN, A. 2017 *Convection in Porous Media*, 5th edn. Springer.
- ORIHARA, H. & TAKIKAWA, Y. 2011 Brownian motion in shear flow: direct observation of anomalous diffusion. *Phys. Rev. E – Statist. Nonlinear Soft Matt. Phys.* **84**, 061120.
- PRATS, M. 1966 The effect of horizontal fluid flow on thermally induced convection currents in porous mediums. *J. Geophys. Res.* **71**, 4835–4838.
- REN, S.Z., SHI, W.F., ZHANG, W.B. & SORENSEN, C.M. 1992 Anomalous diffusion in aqueous solutions of gelatin. *Phys. Rev. A* **45**, 2416.
- STRAUGHAN, B. 2008 *Stability and Wave Motion in Porous Media*. Springer.
- STRAUGHAN, B. & BARLETTA, A. 2024 Asymptotic behaviour for convection with anomalous diffusion. *Continuum Mech. Therm.* **36**, 737–743.
- SUSLOV, S.A. 2006 Numerical aspects of searching convective/absolute instability transition. *J. Comput. Phys.* **212**, 188–217.
- TOLIĆ-NØRRELYKKE, I.M., MUNTEANU, E.-L., THON, G., ODDERSHEDE, F.L. & BERG-SØRENSEN, K. 2004 Anomalous diffusion in living yeast cells. *Phys. Rev. Lett.* **93**, 078102.
- VALDÉS-PARADA, F.J. & SÁNCHEZ-VARGAS, J. 2024 Upscaling mass adsorption and momentum transport in the crown of trees. *Phys. Fluids* **36**, 033303.
- WU, J. & BERLAND, K.M. 2008 Propagators and time-dependent diffusion coefficients for anomalous diffusion. *Biophys. J.* **95**, 2049–2052.